ISSN 1061-3862, International Journal of Self-Propagating High-Temperature Synthesis, 2007, Vol. 16, No. 3, pp. 154–168. © Allerton Press, Inc., 2007.

Combustion Joining of Refractory Materials

A. S. Mukasyan and J. D. E. White

Department of Chemical and Biomolecular Engineering, University of Notre Dame, Notre Dame, IN, 46556 USA

e-mail: amoukasi@nd.edu

Received July 30, 2007

Abstract—This paper overviews heterogeneous exothermic reactive systems as they apply to the joining of materials. Techniques that are investigated fall under two general schemes: so-called Volume Combustion Synthesis (VCS) and Self-Propagating High-Temperature Synthesis (SHS). Within the VCS scheme, applications that are considered include Reactive Joining (RJ), Reactive Resistance Welding (RRW), and Spark Plasma Sintering (SPS). Under the SHS scheme, Combustion Foil Joining (CFJ) and Conventional SHS (CCJ) are discussed. Analysis of the relevant works show significant potential, particularly for the RJ, RRW, and CFJ approaches, in the joining of a variety of materials which are difficult, or impossible, to bond using conventional techniques. More specifically, it is shown that these methods can be successfully applied to the joining of: (i) dissimilar materials such as ceramics and metals and (ii) refractory materials, such as graphite, carbon–carbon composites, W, Ta, Nb, etc.

***Key words*:** Self-Propagating High-Temperature Synthesis, combustion synthesis, refractory materials, joining, welding, soldering

PACS numbers: 81.20.Ka, 81.20.Vj, 06.60.Vz

DOI: 10.3103/S1061386207030089

1. INTRODUCTION

The joining of materials using heterogeneous reactive systems falls under the American Welding Society's *exothermic welding* classification. Using highly exothermic thermite reactions between metal oxides and aluminum is one well-known example [1]. Another relevant technique is exothermically assisted shielded metal arc welding, where chemically active additives (e.g. combinations of aluminum or magnesium powders with hematite) in the electrode material enhance electrode melting and the properties of the joint [2].

In this work, we provide an overview of the joining approaches that involve gas-free combustion reactions, however we do not consider the thermite-type systems. The latter technology, initially developed by Thermit®, has been used for more than 50 years and today it is employed almost exclusively to obtain steels and copper compounds for complex welded unions. A particular interest for this technology is building continuous railway tracks, which have been practically implemented all over the word [3, 4]. Rather, we focus on the application of rapid high-temperature gasless self-sustained reactions for joining similar and dissimilar materials, including refractory metals, ceramics, intermetallics, etc.

The class of exothermic reactions that can be used to produce materials was significantly expanded after the development of an approach called Self-propagating High-temperature Synthesis (SHS), or Combustion Synthesis (CS) [5–7]. Briefly, this method is characterized by the propagation of a high-temperature combustion reaction after the local ignition of a heterogeneous exothermic mixture. In the self-propagating mode, the reaction front moves rapidly in a self-sustained manner leading to the formation of the final solid products without the need for any additional energy (see Fig. 1a). In the so-called Volume Combustion Synthesis (VCS) mode, the entire sample is heated uniformly in a controlled manner until the reaction ignites throughout its

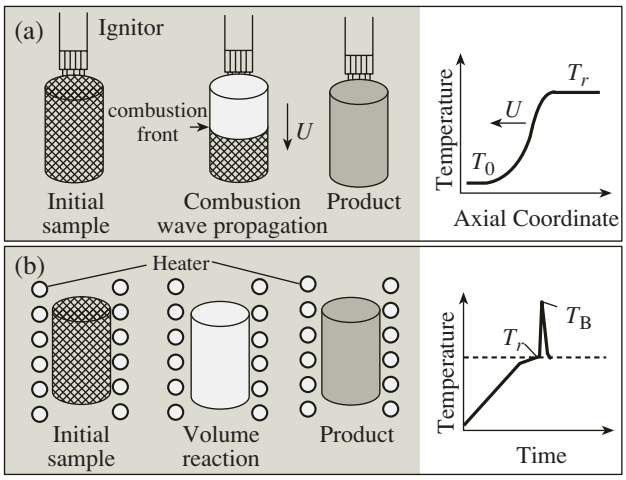

Fig. 1. Schematic of the combustion synthesis method (a) self-propagating mode, (b) volume combustion mode.

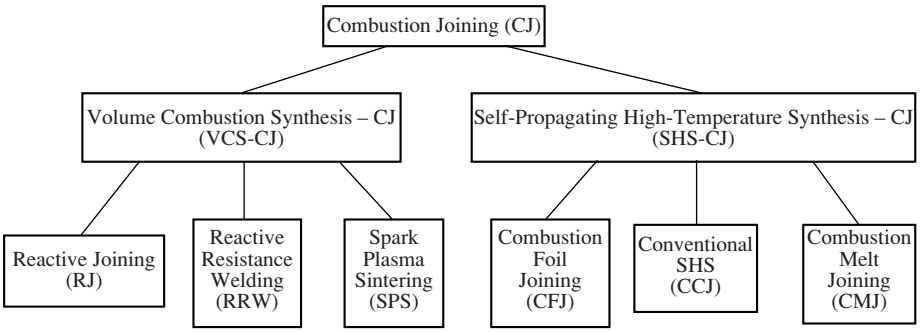

Fig. 2. Suggested classification scheme for combustion joining methods.

volume (Fig. 1b). The VCS mode is typically used for weakly exothermic reactions that require preheating prior to ignition.

In general, such combustion reactions can be described by the stoichiometric equation:

$$\sum_{i=1}^{n} X_i^{s,g} = \sum_{j=1}^{m} P_j^{s,l} + Q,$$

where X_i^s are elemental reaction powders (metals or non metals), X_i^g are the gaseous reactants (e.g. N_2, O_2, H_2), $P_j^{s,l}$ are solid (s) or liquid (l) products, and Q is the heat of reaction. Perhaps the most well known example is the combustion synthesis of titanium carbide: $Ti^s + C^s = TiC^s + 230$ kJ/mol. In the conventional CS scheme, the initial reaction medium is a mixture of heterogeneous powders (i.e. Ti and C), with characteristic sizes in the range of 1–100 microns. Other CS features are high reaction temperatures (for the Ti + C system, $T \approx 3000$°C) and short reaction times (10^{-2}–10 s).

While initially developed for the synthesis of materials and powders, this approach is attracting more and more attention as a tool for joining various substances, which is hereafter referred to as Combustion Joining (CJ). Several CJ schemes for the bonding of different materials, including superalloys, refractory metals (e.g. Mo, Ta), and ceramics have been reported [7–15]. Let us first suggest a classification system for these CJ-based approaches.

2. CLASSIFICATION OF CJ METHODS

The suggested classification scheme is shown in Fig. 2. First, similar to the material synthesis case, these methods can be divided, based on the *method of reaction initiation*, into SHS and VCS combustion joining. In the first scheme, the reaction is locally (in a spot volume of several hundreds of microns) initiated (e.g. by means of a laser or electrically heated metal wire) in the reactive bonding layer, and a self-sustained combustion wave propagates along the reactive media, leading to a high temperature interaction between the layers and chemically "welded" components. The second scheme assumes that the reactive layer is externally preheated to its so-called self-ignition temperature, and thus the reaction is initiated uniformly throughout the entire volume of the layer.

Each of the above approaches has advantages and disadvantages. For example, the SHS-CJ scheme requires essentially no additional energy to make a joint. However, in this case, owing to a finite rate of reaction propagation, it is difficult to reach a uniform temperature distribution along the joining layer. The latter may lead to a joint with a non-uniform microstructure, influencing its properties. This issue becomes even more important if (as is typically performed) an external pressure is applied to the stack to enhance the mechanical property of the joint. As a result, the question of what moment in time to apply the additional pressure arises.

This problem can be partially overcome if the reaction propagates with an extremely rapid velocity (m/s). Such an idea leads to a modification of the SHS-CJ method, where instead of reactive powder mixtures, thin extremely rapid reactive films are used. We call this modified method combustion foil joining (CFJ). Thus, classification of the CJ-based processes can also be suggested based on the *physical nature of the initial reactive media*: heterogeneous porous mixture of powders (conventional SHS-CJ), pore-free foils (CFJ), or even a reactive melt (CMJ). Note, however, that such reaction media can also be used in the VCS scheme.

In the case of VCS-CJ, the reported schemes can be subdivided on the *methods of media preheating* to the ignition temperature. In the first sub-classification, an external furnace is used to heat the whole stack as suggested, for example, in [10], hereafter referred to as *VCS-reactive joining (RJ)*. Typical features of this method are: (i) relatively slow (up to 10^2 °C/min) preheating rate, and (ii) the whole stack, not just the reactive layer, is heated to T_{ig}. It is well known [16] that the ignition temperature for most conventional gasless

Table 1. Materials joined using the Reactive Joining (RJ) method

Material(s) Joined	Reactive Media	Refs.
TiAl	Ti + Al + C	[23]
SiC	Ni + Ti + Al + C	[25]
SiC to Ni-based superalloy	Ni + Ti + Al + C	
NiAl to Fe	Ni + Al (in situ)	[24]
Ni-based superalloy	Ni + Al	[10]
Ni-based superalloy	Ni + Al	[21]
Inconel 600	Ni + Al (in situ)	[22]
NiAl to NiCrAlY/Ni-based superalloy	Ni + Al	[27]
NiCrAlY to Ni-based superalloy	Ni + Cr + Al + Y (in situ)	
NiAl to Ni-based superalloy	Ni + Al (in situ)	[13]
C–C composites	B + C + $TiSi_2$	[28]
TiAl	Ti + Al	[11]

mixtures is equal to the melting point of the least refractory compound (more precisely, the eutectic temperature). Thus, it could be difficult to reach T_{ig} for compositions with refractory reactants. Also, because of the slow heating rate, VCS-RJ requires a long duration, suggesting solid-state reactions (before ignition) could occur and have a significant impact on the composition of the joining layer. Such a modification of the composition can decrease the combustion temperature and the amount of liquid phase that develops after ignition. The latter may lead to a final joint with poor mechanical properties.

Another VCS-CJ approach contains some features of conventional resistance welding, where the heat required for joining is produced by the resistance to the flow of electric current passing through the parts to be welded (Joule heating). This type of material joining, which will be referred to as VCS-*reactive resistance welding (RRW)*, has also been used to join different materials [9, 17–19]. Briefly, a layer of reactive mixture (or foils) is placed between the two materials to be joined. The stack is held in place between two electrodes, which are connected to a DC power supply. DC current is used to uniformly initiate the reaction in the reactive layer. A similar idea was used in the so-called *spark plasma sintering (SPS)* method [20]. However, in SPS, electrical current is important to promote the reaction sintering process, while in the case of VCS-RRW it is used only to uniformly initiate a reaction. Moreover, for many materials it is undesirable to keep electrical current flowing for a long time, as it may lead to degradation in their properties.

Let us overview the results on the joining of different materials using the CJ schemes mentioned above. Focus is placed on the materials that have been welded, the reactive systems used, and the properties of the obtained joints.

3. VCS-COMBUSTION JOINING

3.1. Reactive Joining

As noted above, the RJ method is a sub-classification in which heating by an external furnace is used to initiate a reaction in joining layer. As mentioned above, in this case the components to be joined are held together with a reactive layer in between. In most cases, a significant external pressure is applied to the stack, which is placed in a furnace with a graphite, or similar, heating element under an inert or vacuum atmosphere.

A couple of key features that distinguish this method from the others are: (i) a relatively slow (up to 10^2 °C/min) preheating rate and (ii) the whole stack (not just the reactive layer) is uniformly heated to the processing temperature. In some cases (very slow heating rates), the reaction occurs in the so-called reactive sintering mode. In others, the reactive media ignites upon reaching a specific temperature, T_{ig}.

It has been demonstrated that a variety of materials can be joined by the reactive joining method (see Table 1). Notice that some works deal with joining similar alloys together, while others investigated the bonding of dissimilar materials (e.g. ceramics and alloys). Reported works on the method dealt with Ni-based superalloys and Ni + Al joining layers [10, 21, 22]; TiAl to itself with mixtures of Ti, Al, and C powders [11, 23]; NiAl in situ to Fe [24]; SiC to itself and Ni-based superalloys [25, 26]; NiAl to Ni-based superalloys with Ni, Al, Cr, and Y [27] and Ni, and Al [13]; and C–C composites [28]. A few of these works add the step of materials synthesis to the method [13, 24, 27]. That is, one material is simultaneously synthesized while it is joined to another. Such systems are referred to as in situ joining.

Let us consider the most recent results. As noted above, joining of dissimilar materials is an attractive prospect, particularly with refractory compositions such as SiC and Ni-based superalloys [26]. For example, samples of SiC and the GH128 Ni-based alloy were joined with a functionally graded reactive system composed of W, Ti, Ni, and amorphous C powders and a W sheet (see Fig. 3).

Specifically, the machined cylinders (10 mm diameter and 5 mm height) to be welded were polished, cleansed in an ultrasonic bath, and rinsed prior to joining. Then, these SiC and Ni alloy pieces were loaded into the graphite die with a complex multiple reactive layer in between. This layer consists (see Fig. 3) of a uniform compact of W–Ti–Ni–C powder mixture (*1*), a W sheet (*2*), and FGM filler (*3*). The composition of the FGM filler (*3*) at the tungsten sheet side was the same as that of the single filler layer (*1*), and the rest of the filler (*3*) is composed of layers of Ti, Ni, and amorphous carbon. Each layer was designed so that the dif-

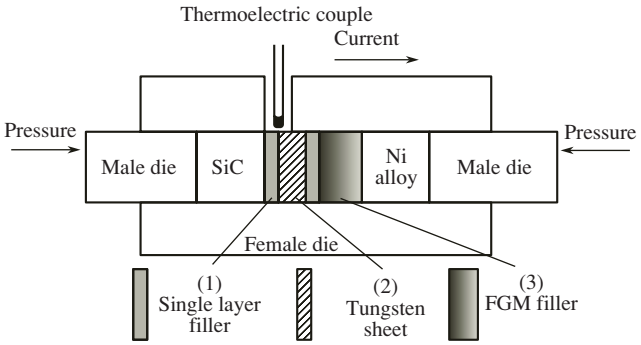

Fig. 3. Schematic map of SHS welding of SiC to Ni-based superalloy.

ference in the coefficient of thermal expansion of the reaction product between neighboring layers was less than 25%. Details of the exact compositions were not given, but are reported to be in future published works. Once assembled in the die, the samples were heated to 1190°C in vacuum and the temperature was held for 10 min. Both the heating and cooling rates were 3°C/s. During the entire process, 25.5 MPa of pressure was applied to the stack.

A micrograph, of the interface of the SiC ceramic and filler material indicates that a reactive layer exists (Fig. 4a: the right side is SiC, and the left is the filler material). EDX analysis pointed out that a large amount of Ti and Ni diffused from the joining materials into the SiC ceramic [25]. At the interface of the W sheet and the filler material (Fig. 4b), a pore-free joining area is also observed. In addition, EDX indicates that Ti and Ni diffused toward the W sheet, as they did at the SiC interface. This diffusion, along with the formation of pore-free joints suggest good bonding at the interfaces.

Several specimens were prepared using tungsten sheets of different thicknesses (0, 0.6, and 1.0 mm). The relative welded fracture strengths were calculated compared to the fracture strength of the initial SiC. As shown in Table 2, the relative strengths range from 48 to 60%. However, it was shown that the fracture occurred in the SiC near the welding seam (~0.5–1.0 mm away), but not on the weld. This is the result of the concentration of residual thermal stresses being highest in this location. It is also apparent that a thicker layer of tungsten improved the welding strength, due to a reduction in thermal stresses at the SiC/reaction products interface.

As mentioned above, in addition to just material joining, researchers have reported on simultaneous synthesis and RJ of materials [13, 24, 27]. Let us consider one of these examples, where NiAl was in situ joined onto Ni-based super-alloys, whose compositions are shown in Table 3 [13]. An equimolar mixture of nickel and aluminum powders were cold-pressed into a $25 \times 4 \times 3$ mm parallelepiped shaped compact using 50 MPa of uniaxial pressure. The compact was then placed on a $25 \times 4 \times 1$ mm super-alloy substrate and inserted into a boron nitride crucible, as shown in Fig. 5. Once placed in a furnace, the joining couple was hydrostatically pressed at 50 MPa in an argon atmosphere and heated at a rate of 90°C/min.

Microanalysis of the joined samples indicates that, during the welding process, a thin layer of the superalloy melted at the interface, followed by a redistribution of aluminum and solidification of the aluminum-rich liquid. The microstructure of the formed NiAl layer was uniform and did not contain intermediate products. The precipitates, which appear as darker spots in the matrix zone between the NiAl and superalloy, had similar compositions independent of the superalloy that was used. A typical micrograph, and compositional analysis, where Hastelloy X was the substrate are shown in Fig. 6 and Table 4, respectively. Near the interface, there is very little porosity and no cracking observed, as the alloy and NiAl have similar expansion coefficients. Note that the matrix is aluminum-rich in the vicinity of the synthesized NiAl. It is clear, from the example that aluminum enrichment occurred in this region due to dissolution of NiAl into the melts, as the Hastelloy did not contain any aluminum (see Table 3).

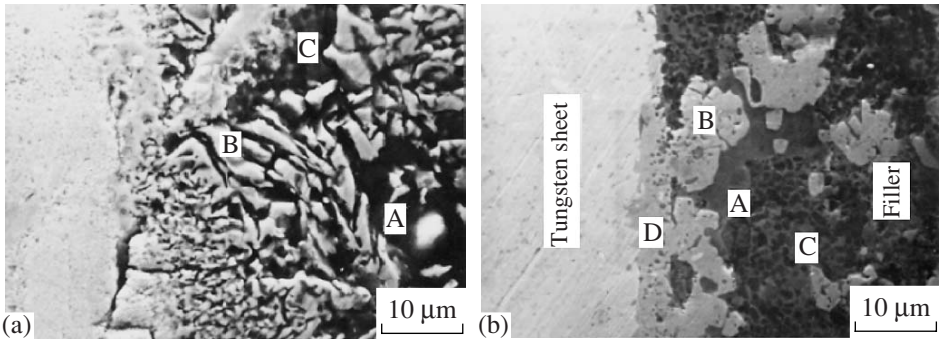

Fig. 4: Microstructure at the interface (a) SiC ceramic and filler material (b) W sheet and filler material.

Table 2. Strength of SHS-welded Ni-based super-alloy and SiC

Sample	Thickness of tungsten sheet, mm	Fracture load, kg	Relative strength, %	Fracture position
1	0	93	48	SiC near welding seam
2	0.6	109	56	SiC near welding seam
3	1.0	117	60	SiC near welding seam

Table 3. Composition of the superalloy substrates used in the RJ method

	Composition in weight percent												
Elements	Ni	Cr	Co	Mo	W	Fe	Ti	Ta	Al	B	Si	C	Mn
Hastelloy X	47.3	22.0	1.5	9.0	0.6	18.5	–	–	–	–	0.5	0.1	0.5
René 77	58.4	14.6	15.0	4.2	–	–	3.4	–	4.3	0.016	0.1	0.1	–
AMI	63.5	7.5	6.5	2.0	5.5	–	1.2	8.6	5.2	–	–	–	–

The examples presented above indicate that the RJ method can be used to *effectively bond* dissimilar materials, including *ceramics and metal alloys*. However, using conventional furnaces, it is difficult to reach the ignition temperature for systems with highly refractory reactants. Furthermore, due to the long duration, it is likely that solid-state reactions (the limiting case being joining by reactive sintering) could have an impact on the final composition, and possibly lead to a joint with high porosity and thus low mechanical properties. Finally, very little is known about the joining mechanism. Further studies are crucial in order to understand and control the RJ process and provide joints with desired properties.

3.2. Reactive Resistance Welding (RRW)

Reactive Resistance Welding (RRW) is an approach that borrows some of the features of conventional resistance welding [29]. A schematic representation of the joining apparatus is shown in Fig. 7. A layer of reactive mixture (*1*) is contained between two disks to be joined (*2*). The stack (*1*, *2*) is held in place between two electrodes (*3*), which are connected to a DC power supply (*4*). DC current is used to uniformly initiate the reaction in the reactive layer. Note that because the resistivity of the porous powder media is typically higher than that of the composite, the Joule heat is primarily evolved in this thin layer. The electrodes are also part of the pneumatic system (*5*) which applies a load to the stack. Once the mixture has reached ignition temperature (T_{ig}), the reaction proceeds rapidly (seconds) in a self-sustained manner reaching a maximum temperature (T_m) on the order of 2800°C. The temperature of the stack can be sensed with a thermocouple or an optical system (*7*). In this particular setup, a computer (*6*) controls the process and monitors process variables.

A typical temperature-time profile for the RRW process is shown in Fig. 8. Note that T_{ig} (~1200°C) was reached in a very short time period (~seconds). At the initiation point, the heating rate in the joining layer rises even more rapidly due to the exothermic combustion reaction, reaching a temperature of about 2000°C in this particular case. After a predetermined Δt_1, the load applied to the stack is increased to promote interaction between the hot reactive mixture and the surfaces of the materials to be joined. After reaction completion the sample was allowed to cool. The whole process requires only about 10 s.

There are relatively few publications on using the RRW method for joining materials [9, 17, 19]. However, the scope of these publications covers different types of compositions (see Table 5). Specifically, this method was used to join extremely refractory materials, e.g. W to Mo, graphite to graphite and to W/Mo, carbon–carbon composites, and super-alloys. A wide variety of highly exothermic reaction mixtures were used, including Ti–C, Ti–B, Ti–C–Ni, Zr–C, and Ti–Ni.

Let us consider a couple of examples. RRW has been demonstrated in the joining of a hard refractory alloy (WC-8Co alloy, $T_m \approx 3000$ K) to Steel 45 (similar to AISI 1045 designation) [17]. The reactive media was composed of a mixture of Ti and Ni powders, pressed into a compact with a relative density of 0.7. It should be noted that prior to joining, the surfaces of the samples were prepped using an abrasive paste and acetone to assure good interactions. Once the alloy, reactive media, and steel were stacked together, a pressure of 10–30 MPa was applied normal to the surfaces to be joined, in a fashion similar to the schematic shown in Fig. 7.

Reactive layer thicknesses were varied from 1.0 mm to 5.0 mm, and the current used to induce the reaction was about 800–1000 A. After joining, the microstructure of the welded materials was investigated with an

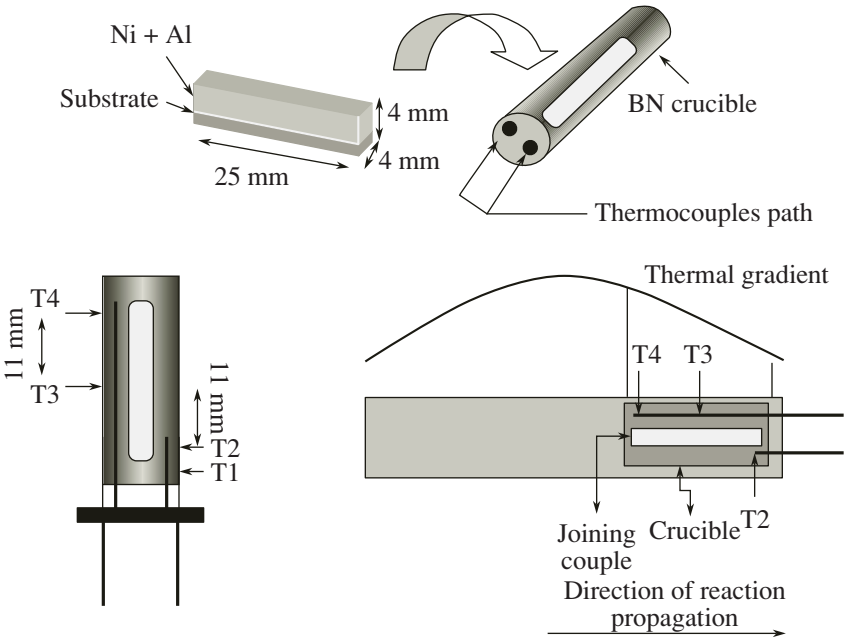

Fig. 5. Schematic representation of the configuration for simultaneous synthesis and joining of NiAl to superalloy.

SEM. Figure 9 shows that dense material formed at the interface of the joint, indicating that good wetting occurred and the molten product (TiNi) had enough time to spread on the joining surfaces. Without any other analysis reported, it is impossible to describe the chemical interactions at these surfaces further.

Additionally, the mechanical properties of joints formed between pairs of hard alloy to steel, hard alloy to hard alloy, and steel to steel were tested. In the case of steel to steel, the material failed in the welding area. But, for the other samples, with the exception of the thickest reactive layer used to join the hard alloy and steel, failure occurred in the hard alloy (see Table 6).

At the University of Notre Dame [19], investigations focused on the joining of carbon–carbon (C–C) composites are currently underway. A novel, computer controlled apparatus has been built for the purpose of investigating the joining of materials with the RRW method (see Fig. 10). Porous compacts of the powder mixture were placed between two cylinders or C–C (see Fig. 11), current was passed through the stack, causing heat to build up in the reactive layer and initiate the Ti + C reaction. After the reaction begins, a high

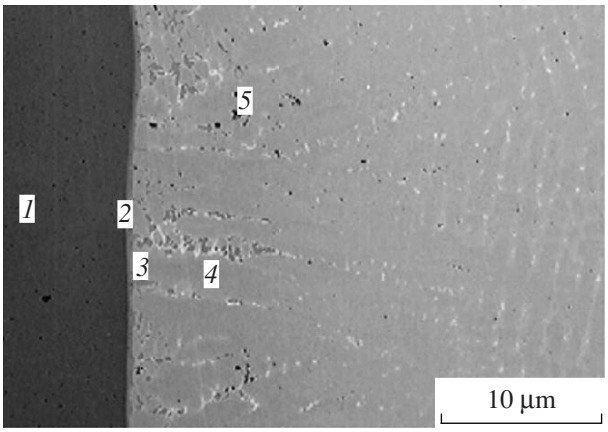

Fig. 6. Microstructure of the NiAl/Hastelloy X joining (300X).

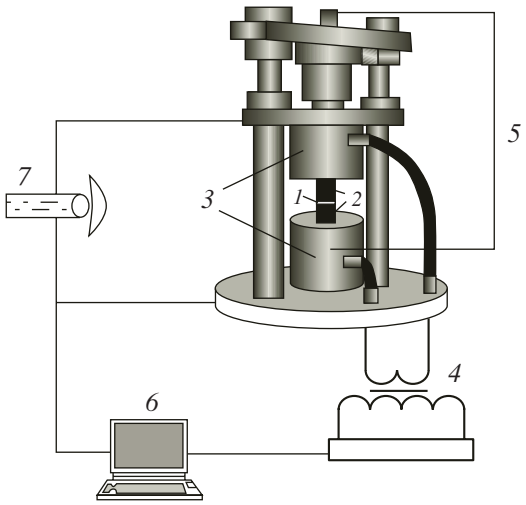

Fig. 7. Schematic diagram of the RRW joining process.

Table 4. EDX analysis of the NiAl/Hastelloy X joining couple

Composition, at %[a]	Ni	Al	Co	Fe	Cr	Mo	W
1—NiAl	50.4	49.6	–	–	–	–	–
2—Interface[b]	55.4	31.7	0.4	5.9	5.7	0.9	–
3—Matrix (5 μm)	51.9	12.8	1.1	13.4	16.8	3.3	–
4—Matrix (50 μm)	52.3	10.8	1.2	15.4	17.5	2.8	–
5—Precipitates	53.8	27.4	0.6	7.6	8.8	1.4	0.2
Hastelloy X	46.9	–	1.5	24.6	24.6	5.4	0.2

Notes: [a] The remainder to 100% corresponds to elements which are not reported.
[b] There is a compositional gradient in this zone.

pressure is applied to the stack (~50 MPa) to squeeze the liquid melt, promote interaction with the C–C surfaces, and enhance the properties of the joint. The entire process only takes on the order of seconds for small samples (~10 mm).

An SEM micrograph, Fig. 12, indicates that the resulting joint is very thin (~10 μm). Also, it was shown that penetration of Ti into the C–C composite does not exceed about 10 μm on either side of the joint. Energy dispersive spectroscopy (EDS) analysis agrees with this assertion, indicating that the joining layer has an essentially uniform phase composition of 75–80 wt % C and 20–25 wt % Ti ($TiC–TiC_{0.8}$), as shown in Table 7.

Tensile strength tests (at $T_0 = 300$ K) of such bonded samples have shown that failure occurred not through the joining layer, but through the C–C. For example, all C–C samples joined using a (Ti + 0.5C) + 8 wt % Ni reaction mixture and an applied pressure greater than 20 MPa, failed at a location relatively far from the joining layer at a tensile stress, $\sigma \approx 10$ MPa. Note that the tensile fracture stress for C–C composites under non-reactive treatment is $\sigma_{C-C} = 10 \pm 1$ MPa. This result indicates a joint with sufficient mechanical properties that are better than that of the bulk material.

One advantage that the RRW method holds over RJ is that it allows one to achieve the ignition temperature very rapidly in the reaction media followed by further temperature increase owing to chemical interaction. Thus, refractory materials (with melting points >1700°C) can be effectively bonded by this method. However, the RRW method suffers from the distinct disadvantage that it can be used primarily only for electro-conductive materials, and samples with large dimensions typically require a large electrical power supply.

3.3. Spark Plasma Sintering (SPS)

The underlying aspects of Spark Plasma Sintering (SPS) are similar to RRW. In fact, from a schematic standpoint, the equipment appears to be almost identical. Notice that the schematic for the SPS process, Figure 13, is very similar to Figure 7 in the RRW section. However, the differences lie in how the DC current is implemented. In SPS, the use of electrical current is important in order to promote the reaction sintering

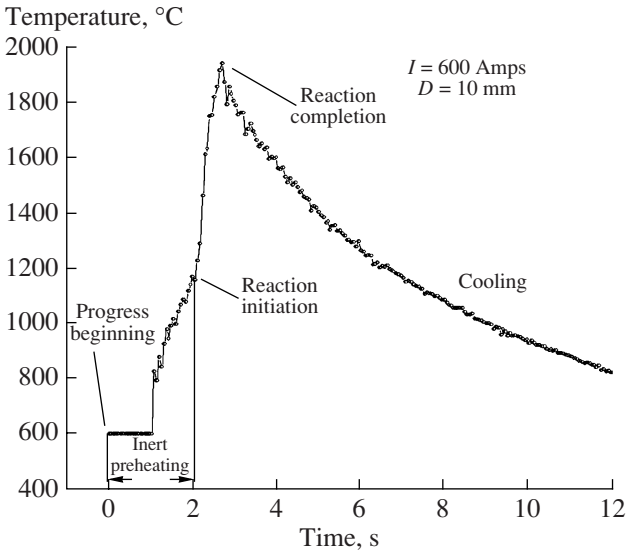

Fig. 8. Typical temperature-time profile of an RRW joining process.

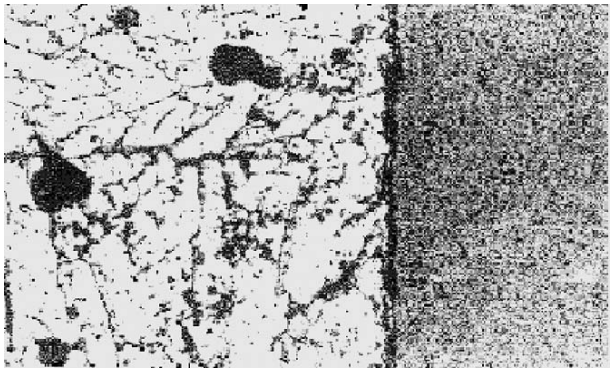

Fig. 9. Microstructure of the welded area between hard alloy and steel.

Table 5. Materials joined with the Reactive Resistance Welding method

Material(s) Joined	Reactive Media	Reference
W and Mo	Mo + B + Cu	[9]
W/Mo and graphite	Ti + C	
Graphite	Ti + C	
WC-8Co and Steel 45	Ti + Ni	[17]
C–C composite	Ti + C	[19]

Table 6. The effect of mixture composition and layer thickness on welding strength

Material	Layer thickness, mm	Weld strength, MPa	Place of failure
Hard alloy–steel	1.0	490	Hard alloy
	1.6	600	Hard alloy
	2.0	420	Hard alloy
	2.5	180	Hard alloy
	2.8	130	Weld area
Hard alloy–hard alloy	1.0	450	Hard alloy
	1.8	310	Hard alloy
Steel–steel	1.0	630	Weld area
	1.2	740	Weld area
	2.0	560	Weld area
	2.7	320	Weld area

process, while in RRW, it is used only to uniformly initiate a reaction. Moreover, the longer duration of electrical current used in SPS can be undesirable in joining some materials, as it may lead to degradation of their properties. Another difference is the fact that in RRW, the electrical current is constant, whereas in SPS the current is pulsed. Finally, current is not just passed through the sample, but also through a die (typically graphite) that surrounds the system of interest during SPS [20].

SPS has received a lot of attention in the last decade, and the number of publications is increasing [20]. Unlike the other methods that have been discussed, most work on SPS is typically focused on the synthesis of materials. A wide range of materials have been synthesized with SPS; catalysts, carbides, cemented carbides, composites, dielectrics, intermetallics, carbon nanotubes, piezoelectrics, shape memory materials, sputter targets, and superconductors just to name a few. However, there are only a few examples on using SPS for joining materials. Notably, joining was demonstrated with nanocrystalline Ni_3Al and Ni_3Al–40 vol % TiC materials [30], and Mo to $CoSb_3$ with a Ti interlayer [31].

The joining of metallic Mo to $CoSb_3$ directly (with no interlayer) is unsuccessful below the decomposition temperature of $CoSb_3$ (875°C). For this reason, an intermediate layer of Ti has been selected, as it has a similar thermal expansion coefficient. Joining was achieved in a two-step SPS process. First, a Ti powder compact was sintered onto the surface of Mo at 980°C in a graphite die under a pressure of 40 MPa and in a vacuum. Then the Ti surface was polished and cleansed in an ultrasonic ethanol bath. Secondly, $CoSb_3$ powder was sintered onto the Ti surface at 580°C under the same pressure and vacuum. For all samples, shear strength testing resulted in fracture along the Ti–$CoSb_3$ interface, and the average shearing strength was about 58 MPa. For reference, the shear strength of the bulk $CoSb_3$ materials was 80 MPa.

SEM and EPMA analysis observed that at the Ti–$CoSb_3$ interface, two intermediate layers appeared. Closest to the $CoSb_3$, there was a layer (~5 μm) that was composed of Ti and Sb in a 1:1 molar ratio and on the Ti side there was a layer (~1–2 μm) that consisted of all three elements: Ti, Co, and Sb. At the other interface, Mo and Ti, the contents of Mo and Ti changed gradually along a thickness of about 50 μm. Mo and Ti are able to form a solid solution in a wide range of compositions, and the resulting gradual change at the interface results in a strong joint. The electrical potential of the joined sample was completed with the four-point probe method. Figure 14 shows a very smooth potential profile, with no abrupt changes at the interfaces between materials, indicating that the interfacial resistance has been minimized.

Joining and simultaneous sintering of different nanocrystalline materials (Ni_3Al/Ni_3Al–TiC) was

Table 7. Elemental distributions along and normal to the joint layer

Direction relative to joint layer	Position of EDS analysis									
	Element concentration wt %, Ti/C									
Along	1	2	3	4	5	6	7	8	9	10
	76.9/23.1	78.5/21.5	76.7/23.3	80.9/19.1	78.5/21.5	65.5/34.5	73.7/26.3	68.2/31.8	76.0/24.0	76.3/23.7
Normal	11	12	13	14	15	16	17	18	19	20
	9.0/91.0	26.9/73.1	58.7/41.3	76.2/23.8	79.5/20.5	81.3/18.7	73.0/27.0	41.4/58.6	21.3/78.7	8.2/91.8

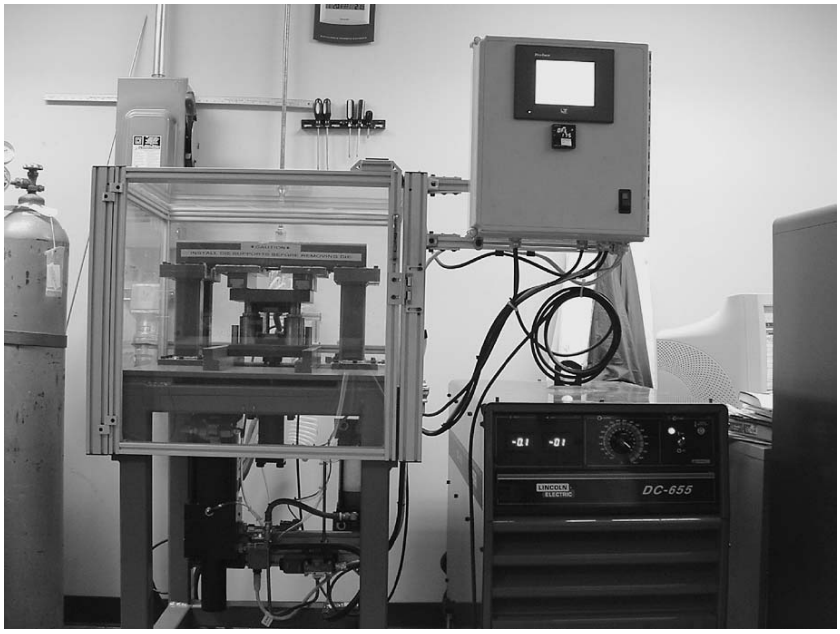

Fig. 10. Novel, computer-controlled apparatus for using the RRW method for joining C–C composites.

achieved by putting compacts of the synthesized powders in the SPS die, followed by heating (under vacuum) to 1100°C at a rate of about 150–200°C/min while a uniaxial pressure of 65–80 MPa was applied [30]. The temperature was held at 1100°C for 5 min, and then cooled at 40°C/min. Good bonding was observed at the interface between the Ni_3Al and Ni_3Al–40 vol % TiC powders, as shown in Fig. 15a. XRD analysis indicated that the joining area consisted of both Ni_3Al and TiC phases; while away from the joint, fully dense materials of the respective desired phases (Ni_3Al and Ni_3Al–40 wt % TiC) were present. EPMA line scans, included in Fig. 15b, confirm the XRD results and suggest that the TiC phase is uniformly distributed in the joining area.

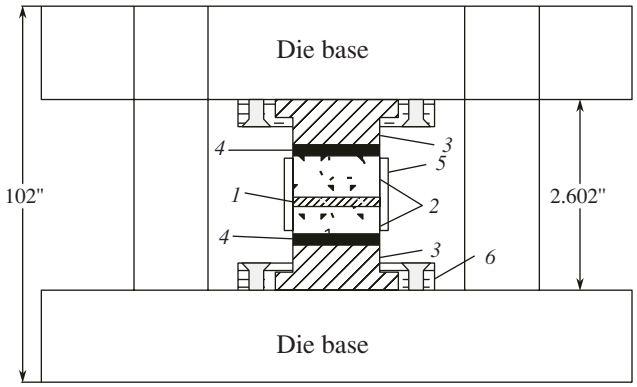

1—Reaction layer; *2*—C–C disks; *3*—dieectric layers; *4*—high current supply; *5*—thermo insulator; *6*—retainer ring

Fig. 11. Die schematic for joining C–C composites using the RRW method.

Based on the above, one may conclude that SPS is an attractive approach for the synthesis of unique materials that cannot be produced without the "catalytic" influence of an electrical field. However, the RRW approach, which was designed specifically for materials welding, is a more powerful tool that allows one to join all compositions bonded by SPS and many more.

4. SHS-COMBUSTION JOINING

4.1. Combustion Foils Joining

The schematics of the CFJ process are shown in Fig. 16. One advantage for the joining process that foils have over powder mixtures is that they are thinner and reactions propagate much faster (~10 m/s, compared to cm/s for powder mixtures) along the pore-free reactive media, thus providing a more uniform temperature distribution in the vicinity of the joint. Furthermore, because only the region immediately surrounding the foil is heated, temperature-sensitive components can be joined effectively. On the other hand, because they are thin, reactive foils only provide high temperature conditions for a very short period of time (<10 ms), and thus are typically used in a manner similar to soldering.

SHS reactive foils are usually prepared by magnetron sputtering of metals (e.g. Ni and Al) onto a substrate [15, 32–35]. Multilayer "thermite" (e.g. CuO_x + Al) foils have also been created [32]. The Weihs and Knio research groups at the Johns Hopkins University completed all of these mentioned works. Other approaches to prepare reactive foils have been investi-

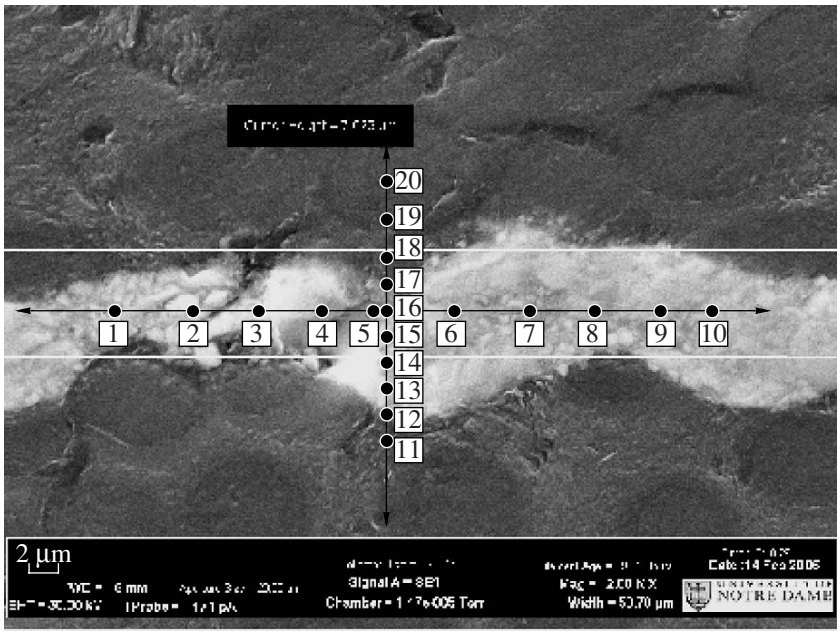

Fig. 12. Micrograph of the typical microstructure of the C–C joining layer.

gated, including pressing alternating layers [36], cold-rolling [37], and hot rolling [38].

As mentioned, the prepared foils are typically coated with a thin layer of braze, such as Incusil ABA (59 wt % Ag–27.25 wt % Cu–12.5 wt % In–1.25 wt % Ti), in order to improve its wetting properties with the solder [34]. The materials to be joined might also be coated with a layer of Incusil ABA braze, or other compositions, such as Au and Ni [15], to enhance wetting at the component surface. Finally, the prepared multilayer foil is sandwiched between the materials to be joined and then it is ignited locally with a spark or some other thermal pulse, as shown in Fig. 16a. The process may take place in a variety of atmospheres, including air, inert (e.g. argon), and vacuum. Also, a pressure is

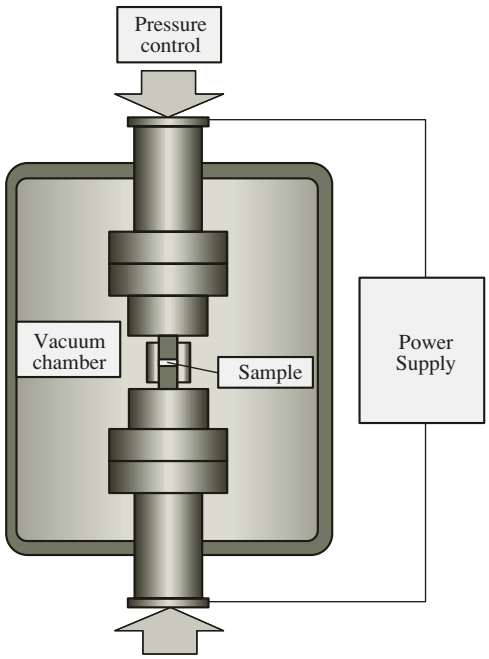

Fig. 13. Schematic of the SPS process.

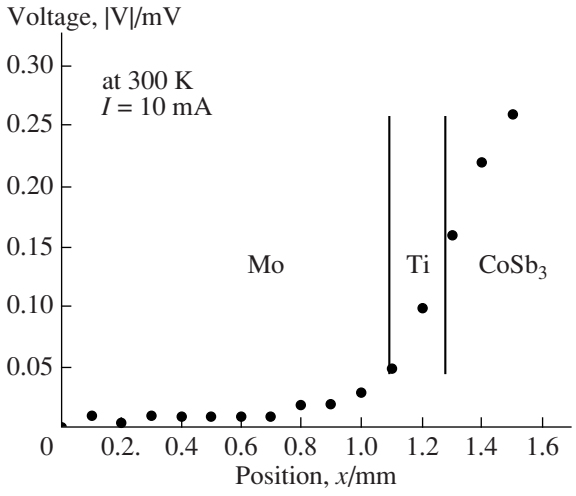

Fig. 14. Potential voltage profile along a joined Mo/Ti/$CoSb_3$ sample.

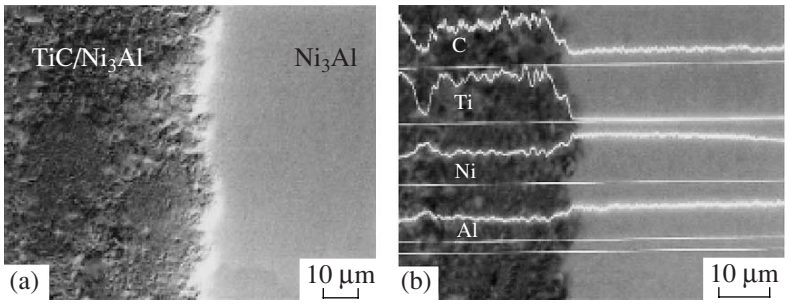

Fig. 15. (a) SEM micrograph and (b) EPMA line scans across the joint interface between nanocrystalline Ni_3Al and Ni_3Al—40 vol % TiC.

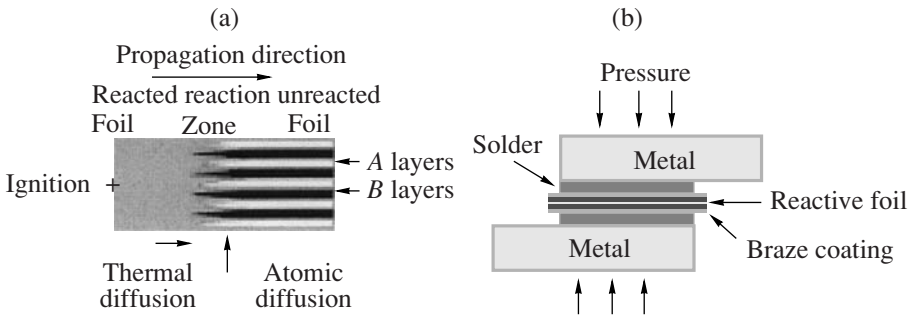

Fig. 16. (a) Schematic of a reaction in a multilayer reactive foil and (b) Schematic showing the reactive joining of two components utilizing reactive foils.

applied to the stack, as it has been shown to improve wetting and enhance the resulting bond [35].

Publications reporting joined materials seem to focus primarily on metals, but due to the rapid heating and cooling rates achievable with CFJ, it has also been demonstrated in joining amorphous metallic glasses without crystallization occurring [39, 40]. The joining of dissimilar materials, such as metals and ceramics, has also been reported using reactive foils [41].

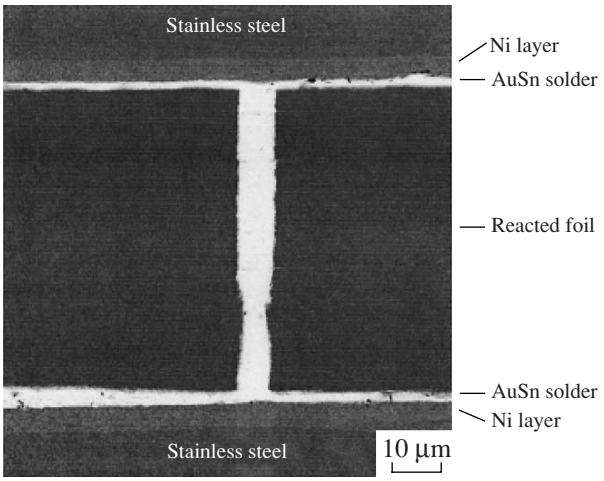

Fig. 17. SEM micrograph of stainless steel components joined using reactive Al/Ni foils and Au–Sn solder.

A couple of example metals include stainless steel [15, 34] and titanium alloys [33]. In these cases (as well as Zr-based glasses) [39, 40], the chosen reactive system was aluminum–nickel (Al–Ni). The foils were magnetron sputtered, alternating Al and Ni layers, and adjusting their thickness (approximately 3 : 2, respectively) in order to ensure a 1 : 1 atomic ratio. For example, a reactive foil (70 to 170 μm thick) was sandwiched between two 25 μm-thick pieces of AuSn solder, and then placed between two 25 mm thick stainless steel specimens to be joined. An external pressure of 100 MPa was applied to the assembled stack during the joining process. For comparison, stainless steel specimens were also joined in a furnace, clamping one piece of AuSn solder between two stainless steel pieces and heating above the melting temperature of the solder.

An SEM micrograph in Fig. 17 suggests that the solder layers completely melted and were squeezed by the applied pressure into cracks that developed in the reacted foil products, further enhancing the properties of the joint. The solder layer was initially 25 μm, and in the joined sample it has been reduced to just a few microns. Thus, it seems that wetting has been sufficiently enabled, and even higher melting point solders or brazes could be used with this method.

All of the joined samples were shear tested in an Instron, and some interesting results were reported. The use of foils creates a joint stronger than conventional solder alone. As shown in Fig. 18, the specimens joined in the furnace had shear strengths of about 38 MPa. The shear strength of CF joined materials quickly rises, as the foil thickness increases from 2 to 40 μm. However, there appears to be no significant advantage to thicker foils, as foils with thicknesses between 40 and 190 μm produce joints with average shear strengths of 48 ± 3 MPa.

It can be concluded that CFJ is an effective approach for bonding of materials that are not highly refractory. Also, note that thin and flexible foils can be used to join complex surfaces. However, the limited commercial availability and preparation of complex reactive foils-braze compositions makes this technology relatively expensive and somewhat less attractive for many uses.

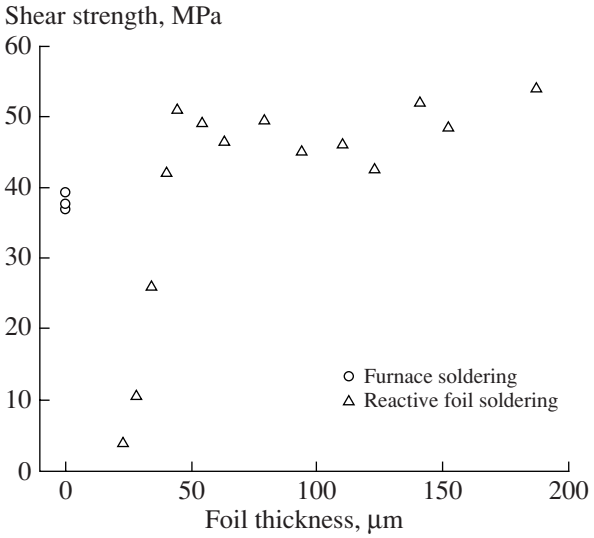

Fig. 18. Shear strength of stainless steel joined with Al/Ni reactive foils as a function of foil thickness.

4.2. Reactive Powder Mixtures

Very few publications were found on the use of the SHS method to join materials with reactive powder mixtures. In fact, works that report "SHS" and "joining" typically fall into the VCS joining scheme, particularly reactive joining (RJ). Let us first consider a recent result on using SHS-CJ to synthesize and join a refractory coating onto a metal surface.

Using a thermite-type system, a ceramic was synthesized and joined to the walls of a metal pipe, forming a composite [42]. In order to accomplish this, carbon steel pipes were picked with acid, and then one end was sealed with aluminum cape. Mixtures of $TiO_2 + C + Al$ and $CrO_3 + Al$ were prepared according to the following stoichiometric reactions:

$$CrO_3 + 2Al \longrightarrow Al_2O_3 + Cr + 1094\ kJ,$$

$$3TiO_2 + 3C + 4Al \longrightarrow 2Al_2O_3 + 3TiC.$$

These two systems, along with Ni, were used to fill the pipes (Table 8). The combustion reaction was initiated using an electrically heated tungsten wire. SEM analysis indicated that the final product has a three-layer structure composed of a steel substrate, intermediate alloy, and ceramic lining. There are carbides (TiC) in the form of particles or fine dendrites distributed in the intermediate alloy, with an atomic ratio of Ti : C = 1.0 : 0.34.

Mechanical properties determined for each sample included Vickers hardness, compressive strength, and compressive shear strength. It was noticed that the increasing content of nickel in the reactive mixture resulted in a denser product structure and a higher Vickers hardness. It is also shown that the maximum strengths for sample A4, as shown in Table 9, are connected with the joining layer microstructure, as well as the content and distribution of the titanium carbide phase.

The SHS-CJ method has also been developed and used [43, 44] in order to join refractory carbon-based materials for applications under extreme conditions, including high temperatures (1600–2000°C), and aggressive chemical environments. This method allows one to cover the surfaces of industrial furnaces, such as those used for high-temperature treatment of sulfur-

Table 8. Composition of combustion systems for SHS coating in steel pipes

Samples	%		
	$CrO_3 + Al$	$TiO_2 + C + Al$	Ni
A1	75	19	6
A2	75	16	9
A3	75	13	12
A4	75	10	15
A5	75	7	18

Table 9. Mechanical properties of SHS-produced composite pipes

Sample	Porosity, %	Vickers hardness, GPa	Compressive strength, MPa	Compressive shear strength, MPa
A1	10.8	15.0	332	26.4
A2	8.3	16.6	376	30.2
A3	5.4	17.3	416	34.3
A4	4.2	18.7	523	39.8
A5	3.5	19.6	451	36.1

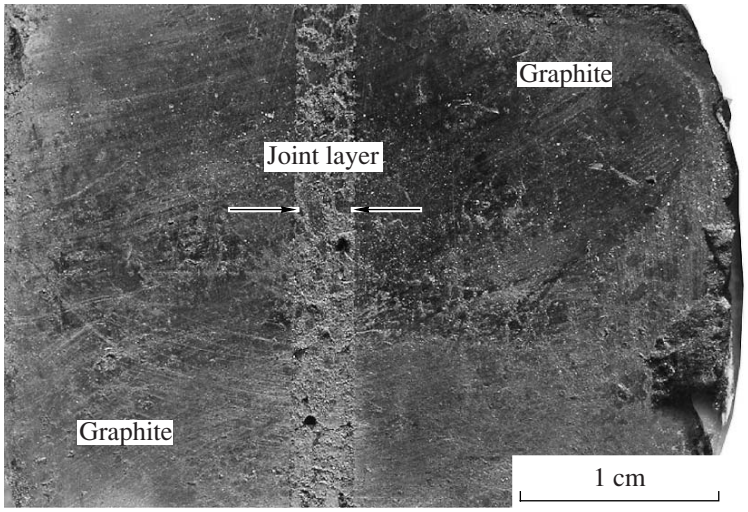

Fig. 19. Joining layer between refractory carbon components using the SHS-CJ method.

containing ores, electrolyte baths for production of alumina and other non-ferrous alloys, blast-furnaces, etc., with carbon tiles. Different types of carbon-based refractory tiles can be joined with this technique. Examples include materials made from conventional coke, graphite, and graphite-silicon carbide composites.

The method is based on the usage of a complex thermite-type reaction, i.e. $4Al + 3SiO_2 + 3C = 2Al_2O_3 + 3SiC$, to make a strong chemically bonded joint between the refractory materials. The main obstacle in using this approach is to avoid the formation of brittle phases such as alumina carbide and silicide, which was overcame by optimization of the reactant particle size and heat-treatment schedule. Also, in order to improve the mechanical properties of the obtained joint, a small amount of a silicon acid solution containing up to 35 wt % SiO_2 with particle size on the order of 20 nm was used. It is important to note that after drying for 4 hours at 50°C, the solution completely converted to the solid state forming an extremely thin SiO_2 nano-layer on the surfaces of the reagents. After the drying process, the joining stack was preheated in a furnace to about 1000°C, at which point reaction initiation occurred. The SHS wave propagates with a velocity ~5 mm/s and maximum temperature ~1700°C. The resulting joining layer (see Fig. 19), while it is porous, exhibits high mechanical properties and chemical stability. XRD analysis confirmed that the layer consists primarily of silicon carbide and alumina. Note that no external pressure was applied to the stack during the bonding process. As it is very simple and inexpensive, this method may be attractive for a variety of large-scale (industrial) applications.

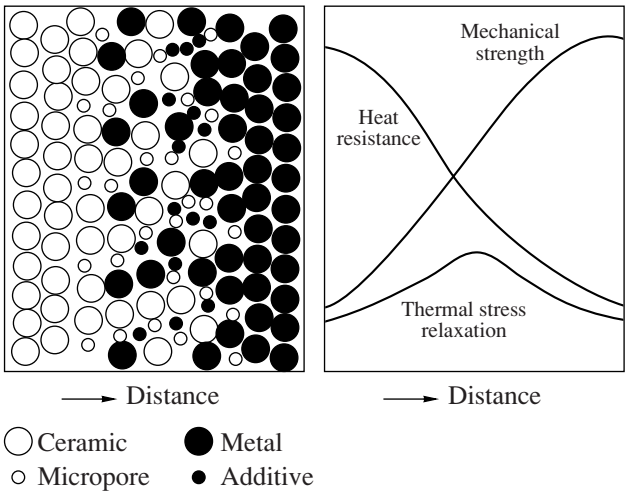

Fig. 20. The Functionally Graded Material (FGM) concept.

It can be concluded that direct SHS-CJ by heterogeneous powder reactive mixtures (except for Thermit® joining, which was mentioned in the Introduction section) has not attracted much attention of scientists and engineers. Presumably, this is a result of the disadvantage that the rate of reaction propagation in such mixtures is relatively slow and hence it is difficult to provide ideal joining conditions.

5. CONCLUDING REMARKS

Several joining approaches that are based on the phenomenon of heterogeneous combustion were briefly overviewed and discussed. No doubt that some of them, such as VCS-RJ, RRW, and CFJ are promising methods for bonding a variety of materials, which are difficult or even impossible to join using other conventional techniques. Two specific applications are of par-

ticular interest and importance: (i) the joining of dissimilar materials such as ceramics and metals and (ii) joining of extremely refractory materials, e.g. graphite, carbon–carbon composites, refractory metals (W, Ta, Nb, etc.).

Finally, it is important to note that the rapid combustion reactions provide a *unique set of conditions* for synthesizing *functionally graded* joining layers. For example, the material structure may have a smooth transition from a metal phase with good mechanical strength on one side, to a ceramic phase with high thermal resistance on the other side, as indicated in Fig. 20. The noteworthy point is that after long-term thermal treatment of the media, all initial graded features are usually dissipated, owing to the diffusion process. However, the short reaction times (~1–10 s) of most CJ systems allow the desired functionally graded material structure to be maintained [45–47]. We believe that this *advantage* of the CJ approach is especially important for the bonding of dissimilar materials that have different coefficients of thermal expansion (CTE). Thus, the formation of a joint with gradually changing properties will alleviate the CTE mismatch problem, which typically leads to mechanical failure.

The next challenge that lies ahead for the research groups involved in the field of combustion joining is to scale-up pilot CJ-apparatuses to effective and commercially available devices.

ACKNOWLEDGMENTS

This work was supported by the Indiana 21st Century Research and Technology Fund.

REFERENCES

1. Ahlert, W., Thermite Welding: Behaviour, Performance, and Examples, *Z. Ver. Deutsch. Ing.*, 1939, vol. 83, pp. 515–518.
2. Allen, J.W., Olson, D.L., and Frost, R.H., Exothermically Assisted Shielded Metal Arc Welding, *Weld. J.*, 1998, vol. 77, p. 277.
3. Meric, C. and Engez, T., Understanding the Thermite Welding Process, *Weld. J.*, 1999, vol. 78, no. 1, pp. 33–36.
4. Meric, C., Atik, E., and Sahin, S., Mechanical and Metallurgical Properties of Welding Zone in Rail Welded via Thermite Process, *Sci. Technol. Weld. Joining*, 2002, vol. 7, no. 3, pp. 172–176.
5. Munir, Z.A. and Anselmi-Tamburini, U., Self-Propagating Exothermic Reactions: The Synthesis of High-Temperature Materials by Combustion, *Mater. Sci. Repts.*, 1989, vol. 3, p. 277.
6. Moore, J.J. and Feng, H.J., Combustion Synthesis of Advanced Materials. II. Classification, Applications, and Modeling, *Prog. Mater. Sci.*, 1995, vol. 39, nos. 4, 5, pp. 275–316.
7. Varma, A., Rogachev, A.S., Mukasyan, A.S., and Hwang, S., Combustion Synthesis of Advanced Materials: Principles and Application, *Adv. Chem. Eng.*, 1998, vol. 24, p. 79.
8. Miyamoto, Y., Nakamoto, T., Koizumi, M., and Yamada, O., Ceramic-to-Metal Welding by a Pressurized Combustion Reaction, *J. Mater. Res.,* 1986, vol. 1, p. 7.
9. Shcherbakov, V.A. and Shteinberg, A.S., SHS Welding of Refractory Materials, *Int. J. SHS*, 1993, vol. 2, p. 357.
10. Messler, R.W. and Orling, T.T., Joining by SHS, in *Adv. Powder. Metall. Part. Mater.*, 1994, vol. 6, p. 273.
11. Uenishi, K., Sumi, H., and Kobayashi, K.F., Joining of the Intermetallic Compound TiAl Using Self-Propagating High-Temperature Synthesis Reaction, *Z. Metallkd.*, 1995, vol. 86, no. 1, pp. 64–68.
12. Matsuura, K., Kudoh, M., Oh, J.H., Kirihara, S., and Miyamoto, Y., Development of Freeform Fabrication of Intermetallic Compounds, *Scr. Mater.*, 2001, vol. 44, no. 3, pp. 539–544.
13. Pascal, C., Marin-Ayral, R.M., and Tedenac, J.C., Joining of Nickel Monoaluminide to a Superalloy Substrate by High Pressure Self-Propagating High-Temperature Synthesis, *J. Alloys Compd.*, 2002, vol. 337, nos. 1, 2, pp. 221–225.
14. Shteinberg, A.S., Merzhanov, A.G., Borovinskaya, I.P., Kochetov, O.A., Ulibin, V.B., and Shipov, V.V., USSR Inventor's Certificate 747 661, 1980.
15. Wang, J., Besnoin, E., Duckham, A., Spey, S.J., Reiss, M.E., Knio, O.M., and Weihs, T.P., Joining of Stainless-Steel Specimens with Nanostructured Al/Ni Foils, *J. Appl. Phys.*, 2004, vol. 95, no. 1, pp. 248–256.
16. Thiers, L., Mukasyan, A.S., and Varma, A., Thermal Explosion in Ni–Al System: Influence of Reaction Medium Microstructure, *Combust. Flame*, 2002, vol. 131, nos. 1, 2, pp. 198–209.
17. Shcherbakov, V.A., SHS Welding of Hard Alloy and Steel, *Key Eng. Mater.*, 2002, vol. 217, pp. 215–218.
18. Shteinberg, A.S. and Knyazik, V.A., Macrokinetics of High-Temperature Heterogeneous Reactions: SHS Aspects, *Pure Appl. Chem.*, 1992, vol. 64, no. 7, pp. 965–976.
19. White, J.D.E., Mukasyan, A.S., La Forest, M.L., and Simpson, A.H., Novel Apparatus for Joining of Carbon–Carbon Composites, *Rev. Sci. Instrum.,* 2007, vol. 78, no. 1, 015105.
20. Munir, Z.A., Anselmi-Tamburini, U., and Ohyanagi, M., The Effect of Electric Field and Pressure on the Synthesis and Consolidation of Materials: A Review of the Spark Plasma Sintering Method, *J. Mater. Sci.*, 2006, vol. 41, no. 3, pp. 763–777.
21. Messler, R.W. and Orling, T.T., Joining Advanced Materials into Hybrid Structures Using Pressurized Combustion Synthesis, in *Advanced Joining Technologies for New Materials II*, 1994, pp. 155–171.
22. Messler, R.W., Jr., Zurbuchen, M.A., and Orling, T.T., Welding with Self-Propagating High-Temperature Synthesis, *Weld. J.*, 1995, vol. 74, no. 10, pp. 37–41.
23. Cao, J., Feng, J.C., and Li, Z.R., Joining of TiAl Intermetallic by Self-Propagating High-Temperature Synthesis, *J. Mater. Sci.*, 2006, vol. 41, p. 4720.
24. Matsuura, K., Ohsasa, K., Sueoka, N., and Kudoh, M., In situ Joining of Nickel Monoaluminide to Iron by Reac-

tive Sintering, *ISIJ Int.*, 1998, vol. 38, no. 3, pp. 310–315.

25. Li, S., Duan, H., Liu, S., Zhang, Y., Dang, Z., Zhang, Y., and Wu, C., Interdiffusion Involved in SHS Welding of SiC Ceramic to itself and to Ni-Based Superalloy, *Int. J. Refract. Met. Hard Mater.*, 2000, vol. 18, no. 1, pp. 33–37.
26. Li, S., Zhou, Y., Duan, H., Qui, J., and Zhang, Y., Joining of SiC Ceramic to Ni-Based Superalloy with Functionally Gradient Material Fillers and A Tungsten Intermediate Layer, *J. Mater. Sci.*, 2003, vol. 38, pp. 4065–4070.
27. Pascal, C., Marin-Ayral, R.M., and Tédenac, J.C., Simultaneous Synthesis and Joining of a Nicraly Layer to a Superalloy Substrate by Self-Propagating High-Temperature Synthesis, *J. Mater. Synth. Process.*, 2001, vol. 9, no. 6, pp. 375–381.
28. Dadras, P., Ngai, T.T., and Mehrota, G.M., Joining of Carbon–Carbon Composites Using Boron and Titanium Disilicide Interlayers, *J. Am. Ceram. Soc.*, 1997, vol. 80, pp. 125–132.
29. Parker, S., in *McGraw-Hill Encyclopedia of Science and Technology*, New York: McGraw Hill, 1997, vol. 19, pp. 488–498.
30. Liu, W. and Naka, M., In situ Joining of Dissimilar Nanocrystalline Materials by Spark Plasma Sintering, *Scr. Mater.*, 2003, vol. 48, p. 1225.
31. Fan, J., Chen, L., Bai, S., and Shi, X., Joining of Mo to $CoSb_3$ by Spark Plasma Sintering by Inserting at Ti Interlayer, *Mater. Lett.*, 2004, vol. 58, p. 3876.
32. Blobaum, K.J., Reiss, M.E., Lawrence, J.M.P., and Weihs, T.P., Deposition and Characterization of a Self-Propagating CuO_x/Al Thermite Reaction in a Multilayer Foil Geometry, *J. Appl. Phys.*, vol. 94, no. 5, pp. 2915–2922.
33. Duckham, A., Spey, S.J., Wang, J., Reiss, M.E., Weihs, T.P., Besnoin, E., and Knio, O.M., Reactive Nanostructured Foil Used as a Heat Source for Joining Titanium, *J. Appl. Phys.*, 2004, vol. 96, no. 4, pp. 2336–2342.
34. Wang, J., Besnoin, E., Duckham, A., Spey, S.J., Reiss, M.E., Knio, O.M., Powers, M., Whitener, M., and Weihs, T.P., Room-Temperature Soldering with Nanostructured Foils, *Appl. Phys. Lett.*, 2003, vol. 83, no. 19, pp. 3987–3989.
35. Wang, J., Besnoin, E., Knio, O.M., and Weihs, T.P., Investigating the Effect of Applied Pressure on Reactive Multilayer Foil Joining, *Acta Mater.*, 2004, vol. 52, no. 18, pp. 5265–5274.
36. Anselmi-Tamburini, U. and Munir, Z.A., The Propagation of a Solid-State Combustion Wave in Ni–Al Foils, *J. Appl. Phys.*, 1989, vol. 66, p. 5039.
37. Bordeaux, F. and Yavari, A.R., Ultra Rapid Heating by Spontaneous Mixing Reactions in Metal–Metal Multilayer Composites, *J. Mater. Res.*, 1990, vol. 5, p. 1656.
38. Oh, J., Lee, W.C., Pyo, S.G., Park, W., Lee, S., and Kim, N.J., Microstructural Analysis of Multilayered Titanium Aluminide Sheets Fabricated by Hot Rolling and Heat Treatment, *Metall. Mater. Trans. A*, 2002, vol. 33, no. 12, pp. 3649–3659.
39. Swiston, A.J., Besnoin, E., Duckham, A., Knio, O.M., Weihs, T.P., and Hufnagel, T.C., Thermal and Microstructural Effects of Welding Metallic Glasses by Self-Propagating Reactions in Multilayer Foils, *Acta Mater.*, 2005, vol. 53, no. 13, pp. 3713–3719.
40. Swiston, A.J., Hufnagel, T.C., and Weihs, T.P., Joining Bulk Metallic Glass Using Reactive Multilayer Foils, *Scr. Mater.*, 2003, vol. 48, no. 12, pp. 1575–1580.
41. Multilayer Foil Enables Ignition, Joining of Dissimilar Materials, *Adv. Mater. Process.*, 2006, vol. 164, p. 8.
42. Zhang, L., Zhao, Z.M., Wang, J.J., Yan, S., and Cao, J.R., Joining between Ceramics and Metal in Composite Pipes Fabricated by the SHS Metallurgical Process, *Key Eng. Mater.*, 2005, vols. 280–283, pp. 887–890.
43. Mansurov, Z.A., Dilmukhambetov, E.E., Ismailov, M.B., Fomenko, S.M., and Vongai, I.M., New Refractory Materials on the Basis of SHS Technology, *La Chimica et l'Industria*, 2001, vol. 83, pp. 1–6.
44. Umarov, N.K., Vongai, I.M., Abdulkarimov, P.G., and Dilmukhambetov, E.E., Macrokinetics of the SHS Process in the Oxide-Based Systems with Shungite, in *2nd International Symposium on Combustion and Plasma Chemistry*, Almaty, Kazakhstan, 2003, pp. 254–257.
45. Koizumi, M., Functionally Gradient SHS Materials, *Int. J. SHS,* 1992, vol. 1, p. 103.
46. Miyamoto, Y., State of the Art in R and D of SHS Materials in the World, *Int. J. SHS*, 1999, vol. 8, p. 375.
47. Dumont, A.L., Bonnet, J.P., Chartier, T., and Ferreira, J.M.F., $MoSi_2/Al_2O_3$ FGM: Elaboration by Tape Casting and SHS, *J. Eur. Ceram. Soc.*, 2001, vol. 21, no. 13, pp. 2353–2360.